Novel Pathogenic Mucorales Identified by Silkworm

Subjects: Mycology | Microbiology | Biology

Contributor: Suresh Panthee

Mucormycosis, a rare but highly fatal infection, is caused by fungi of the order Mucorales. Due to their ubiquitous nature, reduced susceptibility to antifungals, acid tolerance, and ability to infect immunocompromised patients through rapid dissemination, these fungi have been frequently reported to infect the COVID-19 patients. In order to develop strategies to overcome mucormycosis, it is essential to understand and identify novel Mucorales present in the environment.

Mucorales COVID-19 opportunistic infection silkworm animal-model

1. Introduction

Fungi help maintain the diversity of the ecosystem and are critical to nutrient-cycling by degrading dead organic materials [1]. In nature, fungi with agricultural, ecological, economic, biotechnological, and medical importance have been identified. On the other hand, fungi can also cause human infections. Invasive fungal diseases account for a majority of complications among immunocompromised patients worldwide [2]. Fungi of the order Mucorales cause mucormycosis, a rare but highly fatal fungal infection. They can cause cutaneous, rhino-orbital, pulmonary, rhino-cerebral, and disseminated bloodstream infections; the severity and prognosis largely depend upon the infection type. The fatality rate is very high [3] with 96% among patients with disseminated infections [4]. The incidence of mucormycosis is rapidly increasing, especially in developing countries like India and Nepal, where Mucorales were mostly found to cause rhino-orbito-cerebral infections. The most recent incidences are observed in COVID-19 patients [5][6][7] or those who recently recovered from COVID-19. Given that the incidence of mucormycosis has been associated with preexisting conditions such as uncontrolled diabetes mellitus, malignancies, trauma, or extended corticosteroids use [4], it is likely that the number of cases with mucormycosis will increase further due to the current COVID-19 pandemic. Primarily found in soil and decaying vegetation, Mucorales are ubiquitous, have reduced susceptibility to most clinically used antifungal agents, and thrive under high acid conditions. Their thermotolerance, however, is greatly varying; some, such as *Rhizopus microspores* thrive at temperatures as high as 50 °C [8], while some, such as *R. sexualis* cannot grow above 25 °C [8]. Based on their thermotolerance, it was previously thought that Mucorales that cannot grow at 37 °C were medically not important. However, case reports and incidences of cutaneous infections caused by *M. hiemalis* [9][10][11][12], which cannot grow at 37 °C [13][14], have been observed. These cases of infections suggested that the fungi that do not grow at 37 °C are capable of causing superficial infections. Furthermore, invasive mucormycosis rapidly disseminates within the host tissues. Depending upon the infection site, Mucorales interact with specific host receptors and take advantage of the host

physiological conditions to derive nutrients such as iron [15]. Furthermore, Mucorales can store iron in ferritins besides siderophores, further depleting the host of iron and proliferating within the host rapidly [16]. Therefore, patients with diabetes mellitus and COVID-19 are more prone to mucormycosis as these patients have a higher level of free iron in their blood [17][18]. As mucormycosis has been increasingly common, studies on the understanding of their pathogenesis as well as identifying emerging virulent strains are of top priority.

2. Taxonomy and Phylogenetic Analysis

We isolated four fungal strains from plant sources and attempted to identify them (**Table 1**). BLAST analysis of the LSU rRNA region showed that strains 1-3, 5-3, and S286-1101 were related to *Mucor orantomantidis* (accession no: NG_067828.1) with the percentage identity of 95.4% (641/672 bp), 95.4% (641/672 bp), and 97.2% (651/670 bp), respectively. Strain 827-14 was 96% (624/650) identical to *Backusella lamprospora* CBS 118.08 (accession no: NG_058650.1). This result was consistent with the constructed phylogenetic tree using MEGA X [19], where we found that strains 1-3, 5-3, and S286-1101 were claded with *M. orantomantidis*, and strain 827-14 was claded with *B. lamprospora* (**Figure 1**). These findings suggested that these strains were novel species belonging to *Mucor* (1-3, 5-3, and S286-1101) and *Backusella* (827-14). The taxonomic assignment of these strains was further confirmed by the phylogenic tree using ITS sequences, another locus used frequently for the taxonomic demarcation of Mucorales [13]. ITS analysis showed that *Mucor* strains were claded with *M. orantomantidis* (**Figure 2**a) and *Backusella* sp. 827-14 claded with *B. lamprospora* (**Figure 2**b). The phylogenetic tree was reconstructed using MAFFT [20] and RAxML [21] to reveal similar results. Among four strains, we randomly selected *Mucor* sp. 5-3 for whole genome sequencing and SEM analysis.


NG 056283.1 Mucor griseocyanus CBS 116.08
NG 056279.1 Mucor lusitanicus CBS 108.17
NG 056280.1 Mucor ramosissimus CBS 135.65
NG 067371.1 Mucor bainieri CBS 293.63
NG 067365.1 Ellisomyces anomalus CBS 243.57
NG 055735.1 Mucor circinelloides f. circinelloides CBS 195.68
NG 069736.1 Mucor janssenii CBS 205.68
NG 042601.1 Mucor velutinosus ATCC MYA-4766
NG 070580.1 Mucor ctenidius CBS 293.66
NG 055727.1 Mucor racemosus f. racemosus CBS 260.68
NG 057912.1 Mucor mousanensis CBS 999.70
NG 057971.1 Mucor genevensis CBS 114.08
NG 066373.1 Mucor stercorarius CNUFC UK2-1
NG 057918.1 Mucor durus CBS 156.51
NG 063979.1 Mucor abundans CBS 388.35
NG 057917.1 Mucor zonatus CBS 148.69
NG 057916.1 Mucor bacilliformis CBS 251.53
NG 057875.1 Mucor moelleri CBS 444.65
NG 069689.1 Mucor moelleri f. californiensis CBS 402.58
NG 057970.1 Mucor endophyticus CBS 385.95
NG 057968.1 Mucor hiemalis f. hiemalis CBS 201.65
NG 067797.1 Mucor souzae URM 7553
NG 057915.1 Mucor fusiformis CBS 336.68
NG 057969.1 Mucor luteus CBS 243.35
NG 057874.1 Mucor piriformis CBS 169.25
NG 068529.1 Mucor koreanus CNUFC EML-QT1
NG 057876.1 Mucor mucedo CBS 640.67
NG 057922.1 Pirella naumovii CBS 524.68
NG 057933.1 Pirella circinans CBS 962.68
NG 057924.1 Mucor multiplex CBS 110662
NG 057925.1 Mucor megalocarpus CBS 215.27
NG 070842.1 Pilaira moreaui var. caucasica CBS 523.68
NG 057921.1 Mucor flavus CBS 234.35
NG 066156.1 Mucor minutus CBS 586.67
NG 057920.1 Mucor aligarensis CBS 993.70
NG 057919.1 Mucor saturninus CBS 974.68
NG 057923.1 Mucor guilliermondii CBS 174.27
Mucor sp. S286-1101
NG 067828.1 Mucor orantomantidis CNUFC MID1-1
Mucor sp. 1-3
Mucor sp. 5-3
NG 057926.1 Mucor gigasporus CBS 566.91
NG 057913.1 Hyphomucor assamensis CBS 415.77
NG 057914.1 Mucor laxorrhizus CBS 143.85
NG 060268.1 Isomucor trufemiae CCIBt 2328
NG 058813.1 Cokeromyces recurvatus CBS 158.50
NG 069695.1 Benjaminiella poitrasii CBS 158.60
NG 058646.1 Benjaminiella multispora CBS 421.70
NG 069814.1 Benjaminiella youngii CBS 103.89
NG 057932.1 Mycotypha microspora CBS 230.32
NG 064135.1 Mycotypha indica CBS 245.84
NG 064040.1 Mycotypha africana CBS 122.64
NG 057934.1 Poitrasia circinans CBS 153.58
NG 057943.1 Gilbertella persicaria var. persicaria CBS 190.32
NG 057930.1 Mucor zychae var. zychae CBS 416.67
NG 057927.1 Mucor odoratus CBS 130.41
NG 057878.1 Mucor indicus CBS 226.29
NG 057931.1 Mucor falcatus CBS 251.35
NG 057972.1 Mucor variisporus CBS 837.70
NG 060334.1 Mucor caatinguensis URM 7322
NG 057797.1 Helicostylum cordense
NG 057928.1 Mucor azygosporus CBS 292.63
NG 057929.1 Mucor inaequisporus CBS 255.36
NG 057877.1 Mucor amphibiorum CBS 763.74
NG 069778.1 Mucor ardhlaengiktus CBS 210.80
NG 042602.1 Mucor ellipsoideus ATCC MYA-4767
NG 058651.1 Backusella oblongielliptica CBS 568.70
NG 058647.1 Backusella tuberculispora CBS 562.66
Backusella sp. 827-14
NG 058650.1 Backusella lamprospora CBS 118.08
NG 058648.1 Backusella indica CBS 786.70
NG 058649.1 Backusella circina CBS 128.70
NG 056282.1 Rhizopus oryzae CBS 112.07
NG 057873.1 Rhizopus americanus CBS 340.62
NG 059417.1 Rhizopus schipperae ATCC 96514
NG 057870.1 Rhizopus homothallicus CBS 336.62
NG 057871.1 Rhizopus caespitosus CBS 427.87
NG 066155.1 Rhizopus azygosporus
NG 066256.1 Rhizopus microsporus var. chinensis CBS 631.82
NG 064124.1 Utharomyces epallocaulus CBS 112.81
NG 060019.1 Saksenaea trapezispora UTHSC DI 15-1
NG 054826.1 Candida albicans ATCC 18804
0.050

Figure 1. LSU rRNA-based phylogenetic analysis of Mucorales. The LSU rRNA sequence was utilized to infer the evolutionary relationship of the strains. The optimal tree, drawn to scale, with branch lengths in the same units as those of evolutionary distances, with the sum of branch length = 2.44139183, is shown. The percentage of replicate trees in which the associated taxa clustered together in the bootstrap test (500 replicates) are shown next to the branches. After the ambiguous positions were removed for each sequence pair, there were a total of 1552 positions in the final dataset. The novel strains are written in boldface with larger font size.

a

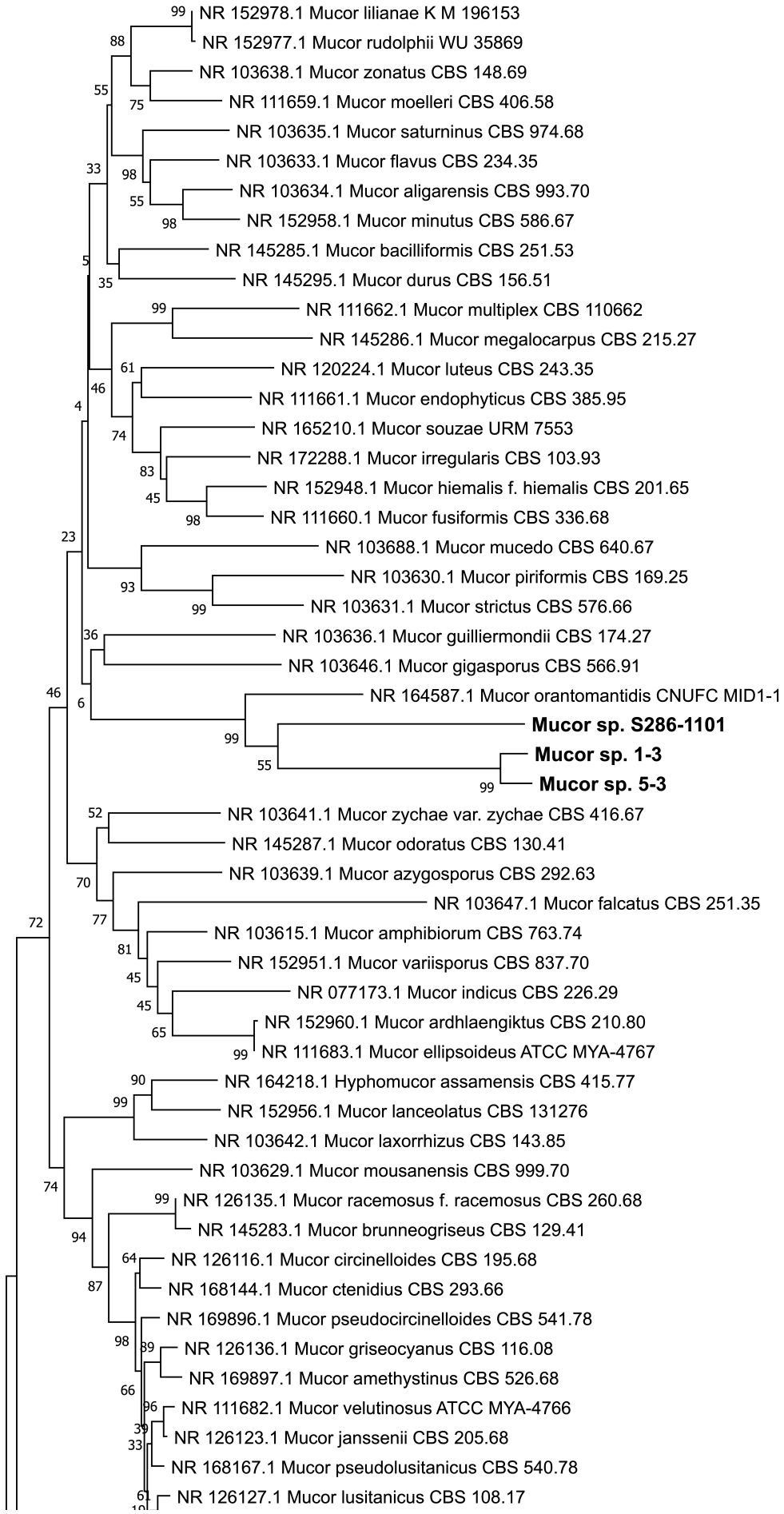
NR 152978.1 Mucor lilianae K M 196153
NR 152977.1 Mucor rudolphii WU 35869
NR 103638.1 Mucor zonatus CBS 148.69
NR 111659.1 Mucor moelleri CBS 406.58
NR 103635.1 Mucor saturninus CBS 974.68
NR 103633.1 Mucor flavus CBS 234.35
NR 103634.1 Mucor aligarensis CBS 993.70
NR 152958.1 Mucor minutus CBS 586.67
NR 145285.1 Mucor bacilliformis CBS 251.53
NR 145295.1 Mucor durus CBS 156.51
NR 111662.1 Mucor multiplex CBS 110662
NR 145286.1 Mucor megalocarpus CBS 215.27
NR 120224.1 Mucor luteus CBS 243.35
NR 111661.1 Mucor endophyticus CBS 385.95
NR 165210.1 Mucor souzae URM 7553
NR 172288.1 Mucor irregularis CBS 103.93
NR 152948.1 Mucor hiemalis f. hiemalis CBS 201.65
NR 111660.1 Mucor fusiformis CBS 336.68
NR 103688.1 Mucor mucedo CBS 640.67
NR 103630.1 Mucor piriformis CBS 169.25
NR 103631.1 Mucor strictus CBS 576.66
NR 103636.1 Mucor guilliermondii CBS 174.27
NR 103646.1 Mucor gigasporus CBS 566.91
NR 164587.1 Mucor orantomantidis CNUFC MID1-1
Mucor sp. S286-1101
Mucor sp. 1-3
Mucor sp. 5-3
NR 103641.1 Mucor zychae var. zychae CBS 416.67
NR 145287.1 Mucor odoratus CBS 130.41
NR 103639.1 Mucor azygosporus CBS 292.63
NR 103647.1 Mucor falcatus CBS 251.35
NR 103615.1 Mucor amphibiorum CBS 763.74
NR 152951.1 Mucor variisporus CBS 837.70
NR 077173.1 Mucor indicus CBS 226.29
NR 152960.1 Mucor ardhlaengiktus CBS 210.80
NR 111683.1 Mucor ellipsoideus ATCC MYA-4767
NR 164218.1 Hyphomucor assamensis CBS 415.77
NR 152956.1 Mucor lanceolatus CBS 131276
NR 103642.1 Mucor laxorrhizus CBS 143.85
NR 103629.1 Mucor mousanensis CBS 999.70
NR 126135.1 Mucor racemosus f. racemosus CBS 260.68
NR 145283.1 Mucor brunneogriseus CBS 129.41
NR 126116.1 Mucor circinelloides CBS 195.68
NR 168144.1 Mucor ctenidius CBS 293.66
NR 169896.1 Mucor pseudocircinelloides CBS 541.78
NR 126136.1 Mucor griseocyanus CBS 116.08
NR 169897.1 Mucor amethystinus CBS 526.68
NR 111682.1 Mucor velutinosus ATCC MYA-4766
NR 126123.1 Mucor janssenii CBS 205.68
NR 168167.1 Mucor pseudolusitanicus CBS 540.78
NR 126127.1 Mucor lusitanicus CBS 108.17

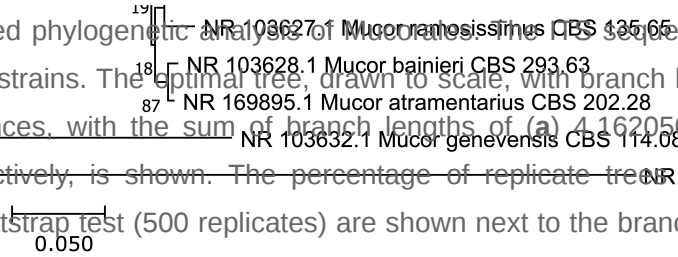

Figure 2. ITS-based phylogenetic analysis of Mucorales. The ITS sequence was utilized to infer the evolutionary relationship of the strains. The optimal tree, drawn to scale, with branch lengths in the same units as those of the evolutionary distances, with the sum of branch lengths of (**a**) 4.16205042 and (**b**) 1.37992789 for *Mucor* and *Backusella*, respectively, is shown. The percentage of replicate trees in which the associated taxa clustered together in the bootstrap test (500 replicates) are shown next to the branches. After the ambiguous positions were removed for each sequence pair, there were a total of 1064 (**a**) and 975 (**b**) positions in the final dataset. The novel strains are written in boldface with larger font size.

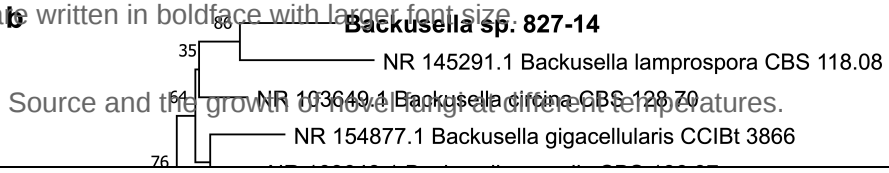

Table 1. Source and the growth of novel fungi at different temperatures.

Strain	Source (Location)	Growth at		
		37 °C (4 Days)	30 °C (4 Days)	4 °C (10 Days)
Mucor sp. 1-3	Plant bud (Chiba, Japan)	−	+++	−
Mucor sp. 5-3	Plant seed (Chiba, Japan)	+	+++	−
Mucor sp. S286-1101	Plant leaf (Saitama, Japan)	+	+++	−
Backusella sp. 827-14	Dead plant leaf (Chiba, Japan)	−	+++	−

3. Analysis of the Mucor Genome Assembly

We have previously used the next-generation sequencing tool for the genomic analysis of various bacteria [22][23] and fungi [24] and have found that compared to the bacterial genome, the fungal genome contains a large number of repeats and is difficult to assemble. We sequenced the *Mucor* sp. 5-3 genome using the Ion PGM System and found that its genome size was 30.8 Mb in size, had a G+C content of 39.26%, and divided into about 17,079 contigs (**Table 2**). This indicated a presence of a large number of repeat elements in the genome. Of note, the same sequencing approach, used for *Candida albicans* TIMM1768 resulted in about 3400 contigs for a 14.5 Mb genome [24]. Besides, combined with a previous study [25], it can be expected that the *Mucor* genome is diverse with a genome size ranging between 30–47 Mb.

Table 2. General features of *Mucor* sp. 5-3 draft genome.

Features	Characteristics
Total reads	5,016,222
Average length (bp)	270
Coverage	44×
Genome size (bp)	30,813,178

Features	Characteristics
Contigs	17,079
Contigs > 1000 bp	6792
Longest contig (bp)	37,105
N_{50}	4436
L_{50}	2075
G + C (%)	39.26

4. Morphological Studies

We found that all the strains grew well on the YPD agar plate at 30 °C when grown under aerobic conditions. However, they had a difference in their growth status at 4 °C and 37 °C. *Mucor* sp. 5-3, and S286-1101 could grow, although slowly, while the other two strains could not grow at 37 °C. At 4 °C, *Mucor* spp. did not show a visible sign of growth; however, *Backusella* showed a faint growth (**Figure 3**). Next, we used *Mucor* sp. 1-3 and *Mucor* sp. 5-3 to check their ability to grow under anaerobic conditions. Incubation for two days at 30 °C after streaking on YPD agar showed that the cells grew as yeast under anaerobic conditions; however, mycelial growth was observed under aerobic conditions (**Figure 4**). Besides, we found that the colony morphology—when visualized with the naked eye—of these two strains on agar plates was similar. When sporangia were observed under a light microscope, a difference was observed among *Mucor* spp. and *Backusella* spp. (**Figure 5**a–d).

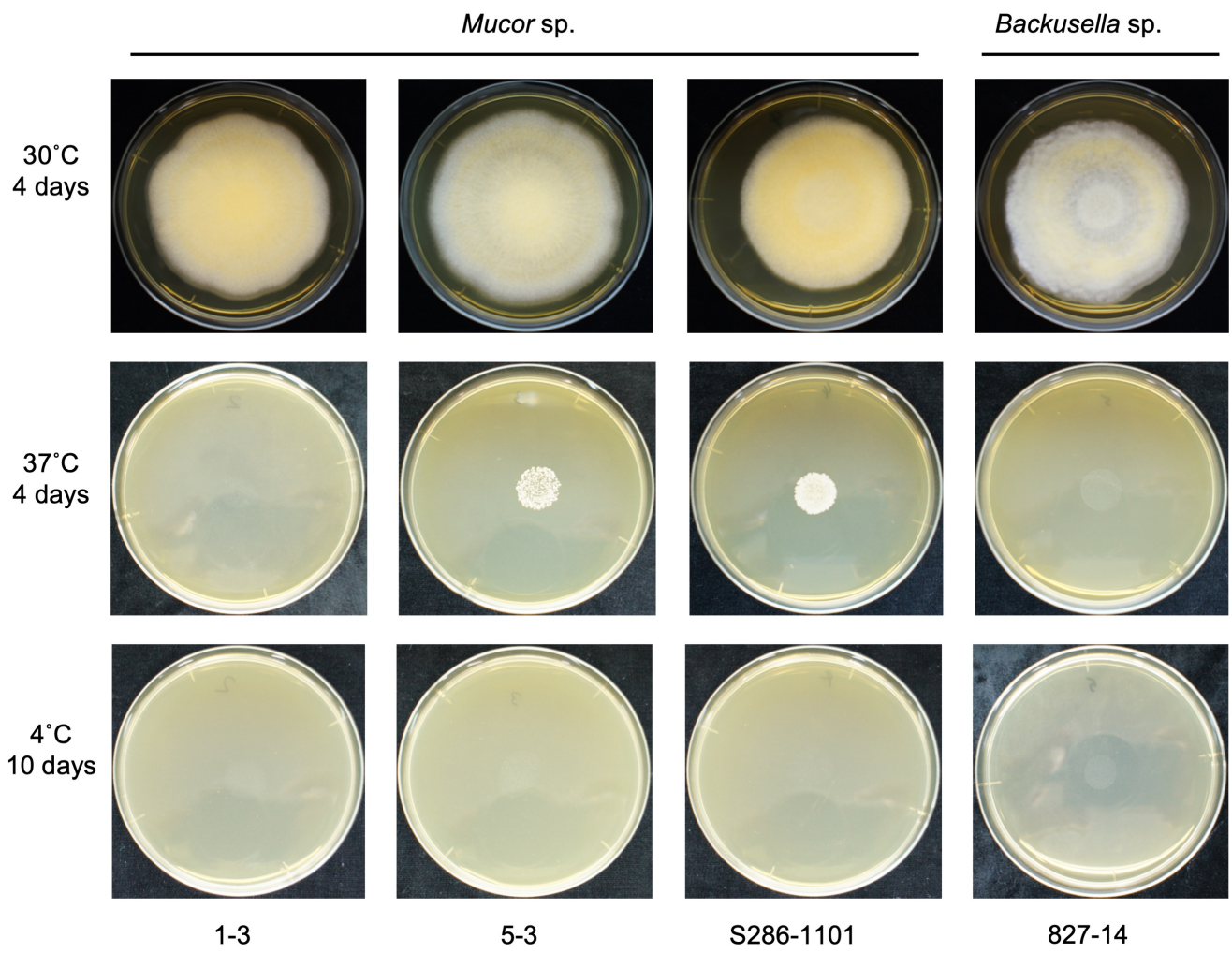

Figure 3. Temperature-specific growth of novel Mucorales. 4.0 × 10^4 spores contained in 40 µL of normal saline were spotted at the center of the YPD agar plates, dried, and incubated at different temperatures for the designated duration before taking a picture.

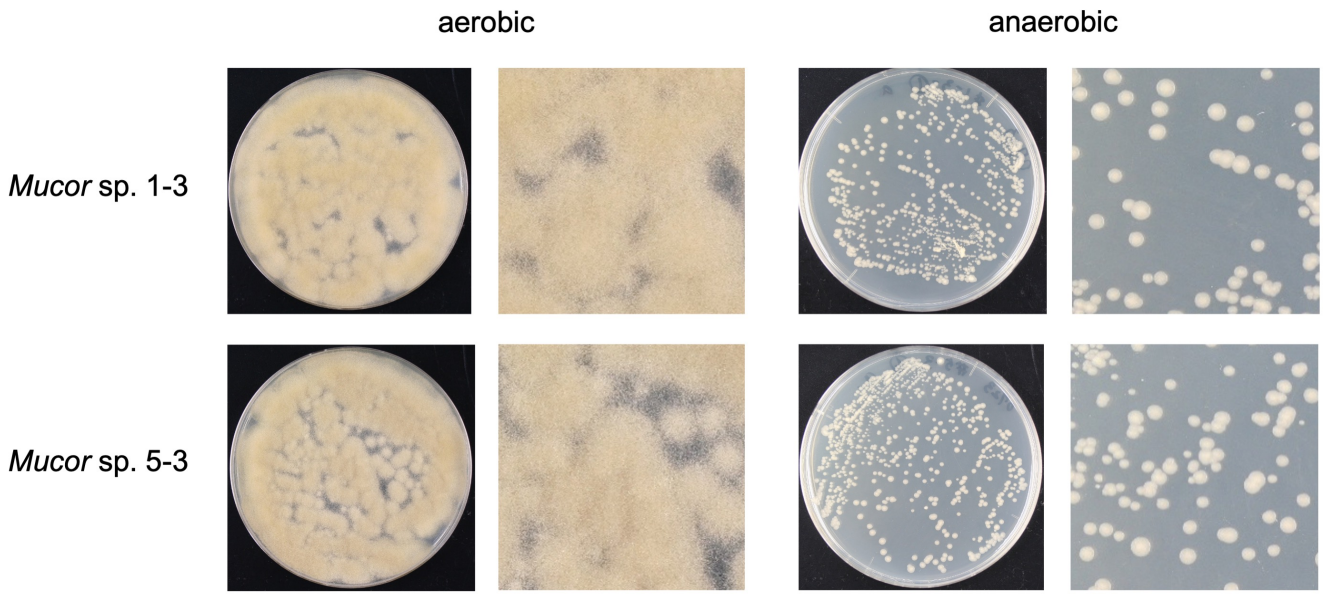

Figure 4. Aerobic and anaerobic growth of *Mucor* sp. 1-3 and 5-3.

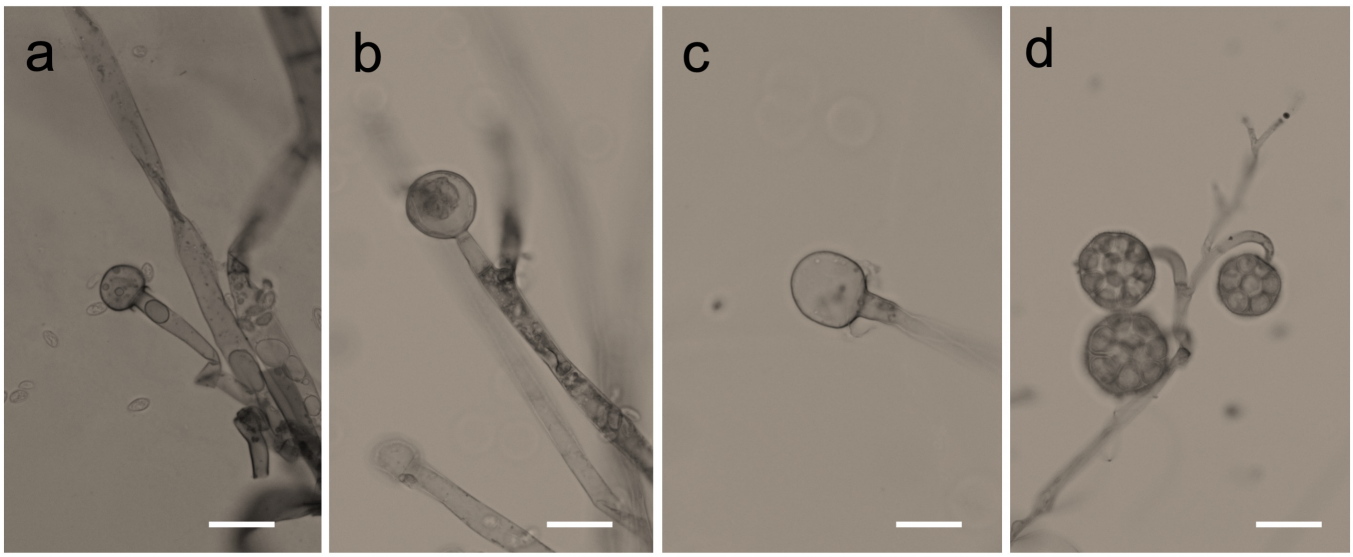

Figure 5. Photomicrographs of Mucorales grown on slide culture. *Mucor* sp. 1-3 (**a**), 5-3 (**b**), S286-1101 (**c**), and *Backusella* sp. 827-14 (**d**). Mucorales were grown aerobically for 4 days. Bars = 20 µm.

5. *Mucor* Morphology under High Resolution

Using *Mucor* sp. 5-3, cell morphology of mycelial growth under aerobic conditions and yeast growth under anaerobic conditions were studied by Scanning Electron Microscope (SEM). Aerobic culture resulted in hyphal growth, where long elongated aseptate hyphae and sporangium were observed (**Figure 6**a,b). Inside the matured

sporangium, a large number of sporangiospores were observed (**Figure 6**c). The tip of sporangiophore harbored columella and collarette (**Figure 6**d). The yeast colonies formed under anaerobic growth were made up of spherical cells of various sizes ranging from 2 to 30 µm in diameter (**Figure 6**e). Multipolar budding cells were observed in large cells (**Figure 6**e,f). Some budding cells had smooth surfaces, whereas some had small golf ball-like shapes (**Figure 6**f). Furthermore, strange cells with cleaved cell surfaces were often observed in large cells (**Figure 6**g). The existence of cells with cleaved surface layers has never been reported before. The significance of these cells in the growth of yeast cells needs to be investigated in more detail in the future.

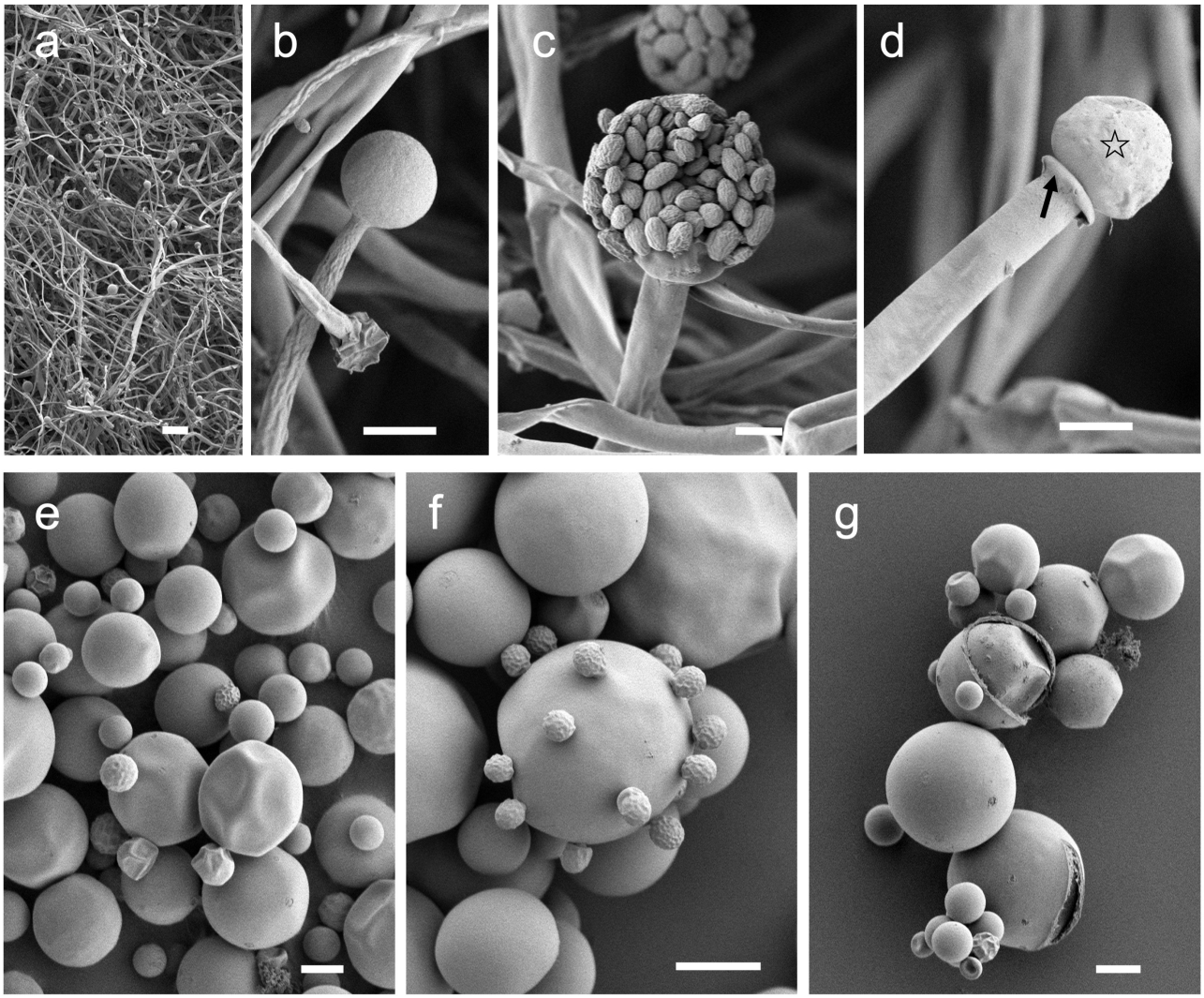

Figure 6. SEM images of aerobic (**a**–**d**) and anaerobic (**e**–**g**) culture of *Mucor* sp. 5-3. (**a**) Low magnification image of mycelium; aseptate hyphae and sporangia. (**b**) Sporangia formed at the tip of the sporangiophore. (**c**) Sporangiospores inside the sporangia. (**d**) Columella (open star) and collarette (filled arrow) were observed at the tip of the sporangiophore. (**e**) Yeast-like colonies are composed of spherical cells of various sizes. (**f**) Multipolar budding found in large cells. (**g**) Cleavage of surface structure is observed in large cells. *Mucor* sp. 5-3 was grown aerobically (**a**–**d**) and anaerobically (**e**–**g**) on a YPD agar plate for 2 days. Bars: (**a**) = 100 µm, (**b**–**g**) = 10 µm.

6. Pathogenicity of Newly Isolated Mucorales

Although various vertebrates and invertebrates are used as animal models to study mucormycosis [26], silkworms were not used to test the pathogenicity of mucoralean fungi so far. Given that the use of the silkworm infection model for the test of pathogenicity of several bacteria and fungi is well established [27][28][29][30], we aimed to evaluate the pathogenicity of novel Mucorales using a silkworm infection model. First, we prepared a suspension of spores and examined the pathogenicity of the suspension without dilution. We found that all silkworms died at 20 h. Next, we prepared a 1/8—fold dilution of spore suspension, injected it into the silkworm, and checked the survival at 15 and 20 h. We found that at 15 h, most of the silkworms were surviving; however, the lethality of these Mucorales was high at 20 h, indicating the ability of these fungi to rapidly kill silkworms. These results indicated the pathogenicity of the spores of newly identified fungi against silkworms. Next, for a quantitative evaluation of pathogenicity, we serially diluted the spores and injected them into the silkworm hemolymph so that each silkworm received 2.5×10^5–1.0×10^3 spores. To confirm the establishment of infection, silkworms were inoculated with 2.5×10^5 heat-killed spores of each strain. Whereas the heat-killed spores were nonpathogenic to silkworms, a dose-dependent killing by live spores was observed (**Figure 7**a–d). We found that with the same dose injected, *Backusella* were more pathogenic compared to *Mucor*.

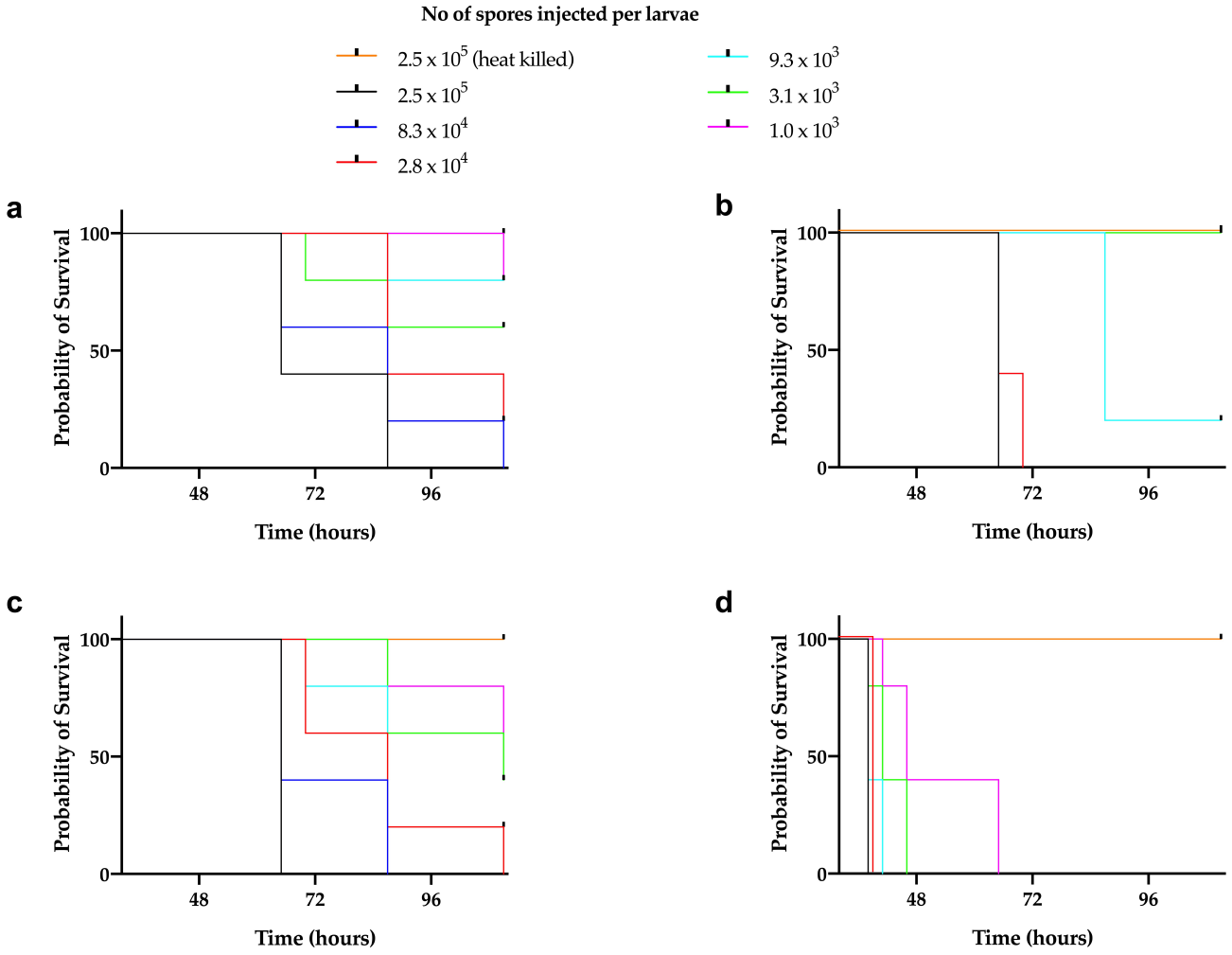

Figure 7. Pathogenicity of Mucorales spores in silkworm. Fifty microliters serially diluted spore suspensions of *Mucor* sp. 1-3 (**a**), *Mucor* sp. 5-3 (**b**), *Mucor* sp. S286-1101 (**c**), and *Backusella* sp. 827-14 (**d**) were injected into the silkworm hemolymph (n = 5). Silkworms were incubated at 27 °C and survival was recorded at various time points.

Next, we tested the ability of these strains to infect mammalian hosts using an immunocompromised mouse model. The result showed that three out of four strains could kill the mouse within four days of the infection suggesting their pathogenicity to mammals (**Figure 8**).

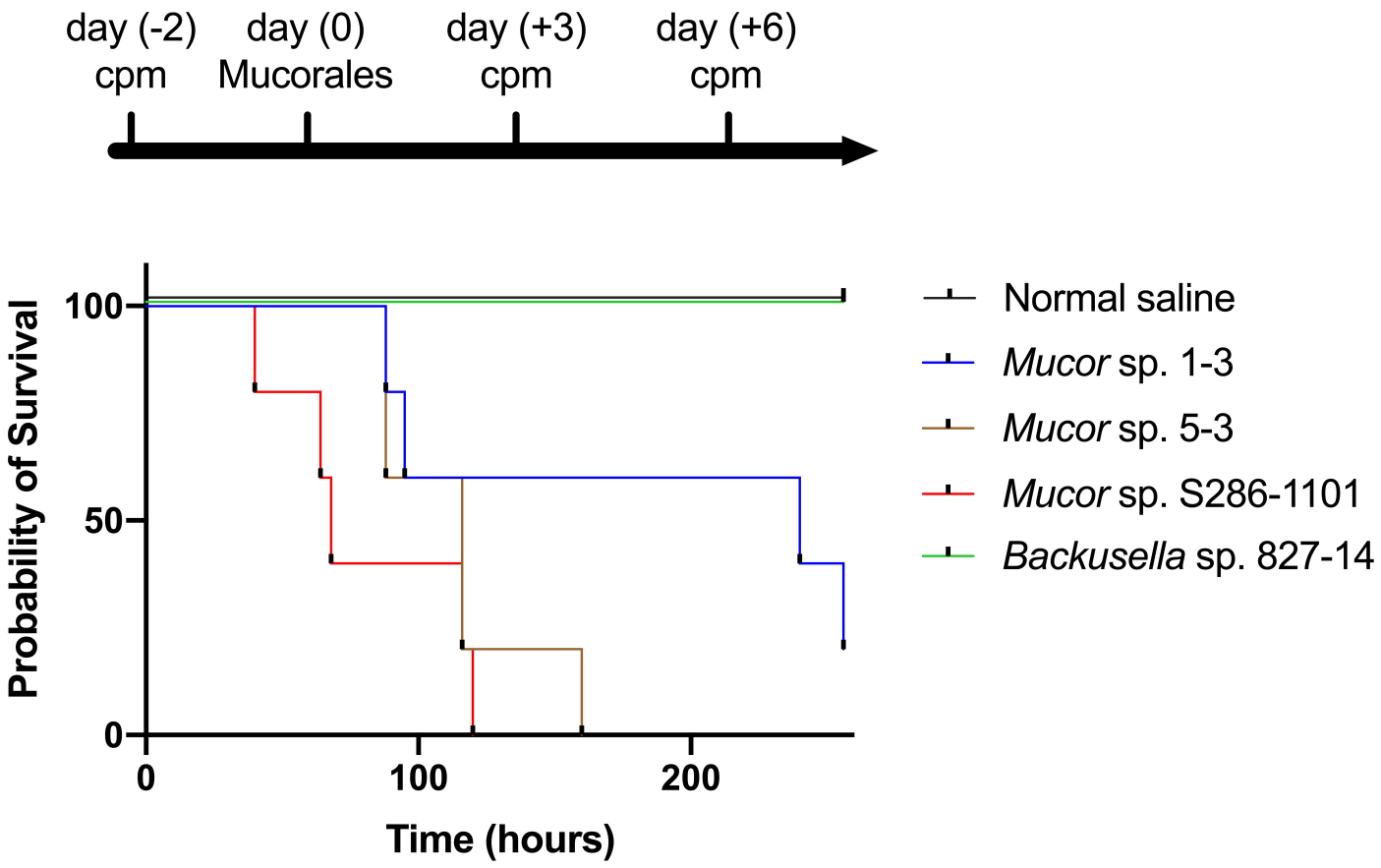

Figure 8. Pathogenicity of Mucorales spores in mice. Four weeks old ICR female mice (n = 5) were immunocompromised by injecting cyclophosphamide (cpm) and injected with 2.0 × 10^8 colony-forming units of Mucorales spores through the intraperitoneal route and survival was recorded at various time points.

References

1. Phookamsak, R.; Hyde, K.D.; Jeewon, R.; Bhat, D.J.; Jones, E.B.G.; Maharachchikumbura, S.S.N.; Raspé, O.; Karunarathna, S.C.; Wanasinghe, D.N.; Hongsanan, S.; et al. Fungal diversity notes 929–1035: Taxonomic and phylogenetic contributions on genera and species of fungi. Fungal Divers. 2019, 95, 1–273.

2. Sanguinetti, M.; Posteraro, B.; Beigelman-Aubry, C.; Lamoth, F.; Dunet, V.; Slavin, M.; Richardson, M.D. Diagnosis and treatment of invasive fungal infections: Looking ahead. J. Antimicrob. Chemother. 2019, 74, ii27–ii37.
3. Roden, M.M.; Zaoutis, T.E.; Buchanan, W.L.; Knudsen, T.A.; Sarkisova, T.A.; Schaufele, R.L.; Sein, M.; Sein, T.; Chiou, C.C.; Chu, J.H.; et al. Epidemiology and outcome of zygomycosis: A review of 929 reported cases. Clin. Infect. Dis. 2005, 41, 634–653.
4. Petrikkos, G.; Skiada, A.; Lortholary, O.; Roilides, E.; Walsh, T.J.; Kontoyiannis, D.P. Epidemiology and clinical manifestations of mucormycosis. Clin. Infect. Dis. 2012, 54 (Suppl. 1), S23–S34.
5. Honavar, S.G. Code mucor: Guidelines for the diagnosis, staging and management of rhino-orbito-cerebral mucormycosis in the setting of COVID-19. Indian J. Ophthalmol. 2021, 69, 1361–1365.
6. Rao, R.; Shetty, A.P.; Nagesh, C.P. Orbital infarction syndrome secondary to rhino-orbital mucormycosis in a case of COVID-19: Clinico-radiological features. Indian J. Ophthalmol. 2021, 69, 1627–1630.
7. Sarkar, S.; Gokhale, T.; Choudhury, S.S.; Deb, A.K. COVID-19 and orbital mucormycosis. Indian J. Ophthalmol. 2021, 69, 1002–1004.
8. Kaerger, K.; Schwartze, V.U.; Dolatabadi, S.; Nyilasi, I.; Kovacs, S.A.; Binder, U.; Papp, T.; Hoog, S.; Jacobsen, I.D.; Voigt, K. Adaptation to thermotolerance in Rhizopus coincides with virulence as revealed by avian and invertebrate infection models, phylogeny, physiological and metabolic flexibility. Virulence 2015, 6, 395–403.
9. Desai, R.P.; Joseph, N.M.; Ananthakrishnan, N.; Ambujam, S. Subcutaneous zygomycosis caused by Mucor hiemalis in an immunocompetent patient. Australas. Med. J. 2013, 6, 374–377.
10. Prevoo, R.L.; Starink, T.M.; de Haan, P. Primary cutaneous mucormycosis in a healthy young girl. Report of a case caused by Mucor hiemalis Wehmer. J. Am. Acad. Derm. 1991, 24, 882–885.
11. De Oliveira-Neto, M.P.; Da Silva, M.; Fialho Monteiro, P.C.; Lazera, M.; de Almeida Paes, R.; Novellino, A.B.; Cuzzi, T. Cutaneous mucormycosis in a young, immunocompetent girl. Med. Mycol. 2006, 44, 567–570.
12. Costa, A.R.; Porto, E.; Tayah, M.; Valente, N.Y.; Lacaz Cda, S.; Maranhao, W.M.; Rodrigues, M.C. Subcutaneous mucormycosis caused by Mucor hiemalis Wehmer f. luteus (Linnemann) Schipper 1973. Mycoses 1990, 33, 241–246.
13. Walther, G.; Wagner, L.; Kurzai, O. Updates on the taxonomy of mucorales with an emphasis on clinically important taxa. J. Fungi 2019, 5, 106.
14. Ribes, J.A.; Vanover-Sams, C.L.; Baker, D.J. Zygomycetes in human disease. Clin. Microbiol. Rev. 2000, 13, 236–301.

15. Alqarihi, A.; Gebremariam, T.; Gu, Y.; Swidergall, M.; Alkhazraji, S.; Soliman, S.S.M.; Bruno, V.M.; Edwards, J.E., Jr.; Filler, S.G.; Uppuluri, P.; et al. GRP78 and integrins play different roles in host cell invasion during mucormycosis. mBio 2020, 11, e01087-20.
16. Ibrahim, A.S.; Spellberg, B.; Edwards, J., Jr. Iron acquisition: A novel perspective on mucormycosis pathogenesis and treatment. Curr. Opin. Infect. Dis. 2008, 21, 620–625.
17. Canturk, Z.; Cetinarslan, B.; Tarkun, I.; Canturk, N.Z. Serum ferritin levels in poorly- and well-controlled diabetes mellitus. Endocr. Res. 2003, 29, 299–306.
18. Cavezzi, A.; Troiani, E.; Corrao, S. COVID-19: Hemoglobin, iron, and hypoxia beyond inflammation. A narrative review. Clin. Pr. 2020, 10, 1271.
19. Kumar, S.; Stecher, G.; Li, M.; Knyaz, C.; Tamura, K. MEGA X: Molecular evolutionary genetics analysis across computing platforms. Mol. Biol. Evol. 2018, 35, 1547–1549.
20. Katoh, K.; Rozewicki, J.; Yamada, K.D. MAFFT online service: Multiple sequence alignment, interactive sequence choice and visualization. Brief. Bioinform. 2019, 20, 1160–1166.
21. Edler, D.; Klein, J.; Antonelli, A.; Silvestro, D. raxmlGUI 2.0: A graphical interface and toolkit for phylogenetic analyses using RAxML. Methods Ecol. Evol. 2021, 12, 373–377.
22. Panthee, S.; Paudel, A.; Blom, J.; Hamamoto, H.; Sekimizu, K. Complete genome sequence of weissella hellenica 0916-4-2 and its comparative genomic analysis. Front. Microbiol. 2019, 10, 1619.
23. Panthee, S.; Paudel, A.; Hamamoto, H.; Ogasawara, A.A.; Iwasa, T.; Blom, J.; Sekimizu, K. Complete genome sequence and comparative genomic analysis of Enterococcus faecalis EF-2001, a probiotic bacterium. Genomics 2021, 113, 1534–1542.
24. Panthee, S.; Hamamoto, H.; Ishijima, S.A.; Paudel, A.; Sekimizu, K. Utilization of hybrid assembly approach to determine the genome of an opportunistic pathogenic fungus, candida albicans TIMM 1768. Genome Biol. Evol. 2018, 10, 2017–2022.
25. Lebreton, A.; Corre, E.; Jany, J.L.; Brillet-Gueguen, L.; Perez-Arques, C.; Garre, V.; Monsoor, M.; Debuchy, R.; Le Meur, C.; Coton, E.; et al. Comparative genomics applied to Mucor species with different lifestyles. BMC Genom. 2020, 21, 135.
26. Jacobsen, I.D. Animal models to study mucormycosis. J. Fungi 2019, 5, 27.
27. Paudel, A.; Panthee, S.; Hamamoto, H.; Grunert, T.; Sekimizu, K. YjbH regulates virulence genes expression and oxidative stress resistance in Staphylococcus aureus. Virulence 2021, 12, 470–480.
28. Paudel, A.; Hamamoto, H.; Panthee, S.; Matsumoto, Y.; Sekimizu, K. Large-Scale screening and identification of novel pathogenic Staphylococcus aureus genes using a silkworm infection model. J. Infect. Dis. 2020, 221, 1795–1804.

29. Panthee, S.; Paudel, A.; Hamamoto, H.; Sekimizu, K. Advantages of the silkworm as an animal model for developing novel antimicrobial agents. Front. Microbiol. 2017, 8, 373.
30. Kaito, C.; Akimitsu, N.; Watanabe, H.; Sekimizu, K. Silkworm larvae as an animal model of bacterial infection pathogenic to humans. Microb. Pathog. 2002, 32, 183–190.